

PRACTICAL RENDEZVOUS SCENARIO FOR TRANSPORTATION MISSIONS TO CIS-LUNAR STATION IN EARTH–MOON L2 HALO ORBIT

Naomi Murakami⁽¹⁾, Satoshi Ueda⁽¹⁾, Toshinori Ikenaga⁽¹⁾, Maki Maeda⁽¹⁾,
Toru Yamamoto⁽¹⁾, and Hitoshi Ikeda⁽¹⁾

⁽¹⁾Japan Aerospace Exploration Agency, 2-1-1 Sengen, Tsukuba, Ibaraki, 305-8505, Japan
⁽¹⁾+81-50-3362-3725, murakami.naomi@jaxa.jp

Abstract: Plans to establish a new international space station in the vicinity of the Moon have drawn attention as a potential gateway for future missions. Assuming that such a station will be constructed, various rendezvous missions will be performed, including logistics flight and crew transportation missions. In the low Earth orbit (LEO), many logistics flight missions have been performed, such as the H-II Transfer Vehicle (HTV) and the Automated Transfer Vehicle (ATV) missions for the International Space Station (ISS), and rendezvous operation technology has been well established. However, in cis-lunar orbits, the dynamics of relative motion are different from those in LEOs, and the GPS-based navigation scheme, which is the key navigation method in LEO rendezvous missions, cannot be applied. Hence, a different type of rendezvous scheme is necessary for application to rendezvous missions in cis-lunar orbits. In this study, we suggest a practical rendezvous scenario for logistics flight missions to the future cis-lunar space station in the Earth–Moon L2 halo orbit and clarify the problems and requirements regarding guidance, navigation, and control (GN&C) for cis-lunar rendezvous.

Keywords: Rendezvous, Cis-lunar station, Earth–Moon L2 halo, GN&C.

1. Introduction

The updated Global Exploration Roadmap delivered by the International Space Exploration Coordination Group (ISECG) outlines strategies for human and robotic exploration to the Moon, asteroids, and Mars [1]. A cis-lunar space station, one of the key elements of this program, would serve as a staging post to access the lunar surface as well as a proving ground for extended-duration crew missions. The location of this cis-lunar space habitat is still under consideration. It will require careful selection with respect to its applicability to coming missions; accessibility to the Moon, asteroids, and Mars; continuous communication with Earth; and orbit transfer and orbit maintenance costs. A lunar distant retrograde orbit (DRO), which has been considered as one of the possible destinations for the captured asteroid in NASA's Asteroid Redirect Mission (ARM) [2], have received considerable attention, mainly because of their long-term stability, which is crucial for a manned mission, particularly when considering off-nominal situations. Another major candidate would be a halo orbit around the Earth–Moon L2 point (hereafter referred to as the EML2 halo orbit). Unlike DROs, EML2 halo orbits exhibit extremely weak stability. However, unstable periodic orbits such as EML2 halo orbits have the significant benefit of having invariant manifolds, which can deliver spacecraft to/from their destinations with low-velocity maneuvers [3, 4]. The use of invariant manifolds in low-cost transfer

strategies between the Sun–Earth and Earth–Moon systems, and even to Mars, has been discussed by many researchers [5, 6]. Although EML2 halo orbits have instability disadvantages, their low-cost transfer capabilities merit evaluation.

If a new station is to be developed in an EML2 halo orbit, continuous crew transportation and logistics flights would be required, as is the case with the International Space Station (ISS) in a low Earth orbit (LEO). Therefore, many vehicles visiting from the Earth would approach and rendezvous with the station. Although rendezvous technologies for LEOs and low lunar orbits (LLOs) have been established for the ISS and Apollo programs, little is known about rendezvous in cis-lunar orbits. For example, we are yet to establish approach trajectory features that will ensure that no collisions occur with the station. Since the gravity field is shallow in cis-lunar orbits, the relative dynamics of proximity motion are almost “straight”; therefore, the “carving” characteristics of LEO trajectories, which govern the ISS safety standards, cannot be used [7]. In addition, the GPS navigation system cannot be directly applied, which is often used as a primary navigation method for far rendezvous operations in LEOs. Another navigation system, such as a ground-based tracking system like NASA’s deep space network (DSN), must be utilized. For cis-lunar rendezvous operations, a different type of rendezvous scheme than that used for LEOs is necessary. Our present study focuses on this point.

The aim of this paper is to develop a practical rendezvous scenario for unmanned logistics transportation missions to a station in the EML2 halo orbit and to identify the problems and requirements regarding guidance, navigation, and control (GN&C) for cis-lunar rendezvous. We suggest a rendezvous trajectory that considers collision safety and a design for a relative navigation system. The scenario is divided into four phases: 1. transfer phase, 2. far-approach phase, 3. rendezvous phase, and 4. proximity phase. For each phase, we address the trajectory design as well as guidance and navigation schemes.

2. Dynamics Model for the EML2 Halo Orbit

2.1. Circular Restricted Three Body Problem

In general, when studying periodic orbits around the Moon and the Earth–Moon Lagrangian points, the motion of the spacecraft is described in the Circular Restricted Three Body Problem (CRTBP). The non-dimensional equation of motion is described as follows:

$$\begin{aligned}\ddot{x} - 2\dot{y} - x &= -\frac{(1-\mu)(x+\mu)}{d^3} - \frac{\mu(x+\mu-1)}{r^3} \\ \ddot{y} + 2\dot{x} - y &= -\frac{(1-\mu)y}{d^3} - \frac{\mu y}{r^3}\end{aligned}\quad (1)$$

$$\ddot{z} = -\frac{(1-\mu)z}{d^3} - \frac{\mu z}{r^3}$$

$$d = |\bar{d}| = \sqrt{(x+\mu)^2 + y^2 + z^2}, \quad r = |\bar{r}| = \sqrt{(x+\mu-1)^2 + y^2 + z^2}$$

where $\mathbf{x} = [x, y, z, \dot{x}, \dot{y}, \dot{z}]$ is a normalized state vector in the Earth–Moon rotating frame centered at the barycenter of the Earth and Moon. The Earth–Moon rotating frame is one in which the x-axis is directed from the Earth to the Moon, the z-axis extends in the direction of angular momentum of the system, and the y-axis completes the right-handed triad. In the following discussion, we use it as the default coordinate system for describing the motion. The mass ratio μ is defined as $\frac{m_2}{m_1+m_2}$, where m_1 and m_2 are the mass of the Earth and Moon, respectively.

2.2. Relative Motion

The nonlinear equation, $\dot{\mathbf{x}} = f(\mathbf{x})$, as represented by Eq. (1), is linearized about a certain periodic orbit:

$$\delta\dot{\mathbf{x}} = A(t)\delta\mathbf{x}$$

where $\delta\mathbf{x}$ is the relative state with respect to the reference orbit, such as the EML2 halo orbit, and $A(t) = \left. \frac{\partial f(\mathbf{x})}{\partial \mathbf{x}} \right|_{\mathbf{x}_{ref}}$ is the Jacobian matrix. $A(t)$ appears in the following form:

$$A(t) = \begin{bmatrix} O_3 & I_3 \\ U_3 & 2\Omega_3 \end{bmatrix}$$

where the constant submatrix Ω_3 is evaluated as follows:

$$\Omega_3 = \begin{bmatrix} 0 & 1 & 0 \\ -1 & 0 & 0 \\ 0 & 0 & 0 \end{bmatrix}.$$

The elements of submatrix U_3 are the second partial derivative with respect to the position states.

The state transition matrix (STM), $\Phi(t, t_0)$, can be expressed in the following form:

$$\delta\mathbf{x}(t) = \Phi(t, t_0)\delta\mathbf{x}(t_0) \quad (2)$$

which satisfies the following conditions:

$$\dot{\Phi}(t, t_0) = A(t)\Phi(t, t_0)$$

(3)

$$\Phi(t_0, t_0) = \mathbf{I}_6.$$

Next, we define a reference vehicle in a certain halo orbit and a visiting vehicle (VV) flying in the vicinity of the reference vehicle. Provided that the VV's relative state at time t_0 is $\delta\mathbf{x}(t_0)$, then the relative state at time $t_1 = t_0 + \Delta t$, $\delta\mathbf{x}(t_1)$ can be obtained using Eq. (2). STM, $\Phi(t, t_0)$, is calculated by integration using Eq. (3), where the Jacobian matrix $A(t)$ is also computed by integrating the initial state of the reference vehicle using Eq. (1). If VV is close enough to the reference vehicle, STM can be approximated as follows [7]:

$$\Phi(t_1, t_0) = \mathbf{I}_3 + \begin{bmatrix} \mathbf{0} & \mathbf{I}_3 \\ \Xi^R(t_0) - \Omega_3 \cdot \Omega_3 & 2\Omega_3 \end{bmatrix} \cdot \Delta t \quad (4)$$

where

$$\Xi(t) = -(c_1(t) + c_2(t))\mathbf{I}_3 + 3c_1(t)[\mathbf{e}_1(t)\mathbf{e}_1^T(t)] + 3c_2(t)[\mathbf{e}_2(t)\mathbf{e}_2^T(t)].$$

$\mathbf{e}_1(t)$ and $\mathbf{e}_2(t)$ are unit vectors directed toward the reference vehicle from the Earth and Moon, respectively. $c_1(t)$ and $c_2(t)$ are represented by $c_1(t) = \frac{1-\mu}{d^3}$ and $c_2(t) = \frac{\mu}{r^3}$, where d and r are the normalized distances of the reference vehicle measured from the Earth and Moon, respectively. This formulation is useful because STM can be estimated using only the station's absolute position information.

3. Cis-lunar Station

3.1. Staging Orbit of the Station

We have assumed that the cis-lunar station flies in an EML2 southern halo orbit with $A_z = 10000$ km, the corresponding period of which is 14.8 days. Figure 1 shows the station orbit as viewed in the Earth–Moon rotating frame centered at the EML2 point. The orbit is calculated with a realistic force model, including the point mass gravity of the Earth, Sun, and Moon.

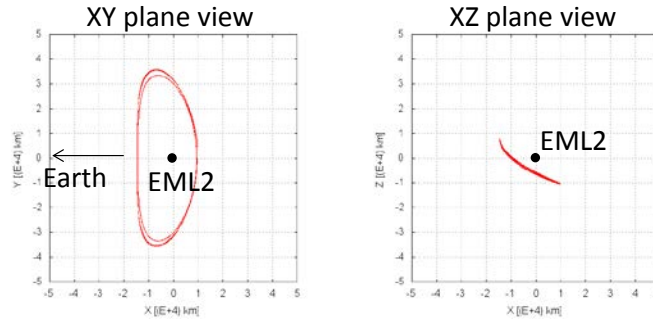


Figure 1. EML2 halo station orbit as viewed in Earth–Moon rotational frame

3.2. Station-based Active Navigation Sensor

In an ISS rendezvous, ISS crews monitor the VV’s status via proximity telemetry and station cameras and execute a command to the VV when any critical anomaly is sensed. However, with respect to the cis-lunar station, we assume that crews may not always be present. Thus, the installation of an active navigation sensor in the station would be preferable to maintain the monitoring capability.

In addition, if the station sends relative navigation data to the VV via proximity communication and the VV could utilize the data as a supportive relative navigation aid, we could simplify the VV design while also maintaining or even improving its safety and robustness.

In this study, we assumed that an onboard radar, having a field-of-view (FOV) of $\pm 30^\circ$, is installed at the station and initiates relative navigation from a relative distance of 200 km.

3.3. Preconditions for the Station

The station’s configuration, nominal attitude, and regular operation such as station-keeping maneuvers, will have a large impact on the rendezvous trajectory design, but these specifications have yet to be fixed. In this study, we assumed that the station’s nominal attitude will be fixed in the Earth–Moon rotating frame and that the station will perform station-keeping maneuvers twice each period as it crosses the x - z plane, as proposed in [8].

For the station to monitor a VV during the rendezvous operation, VV must approach within FOV of the station-based radar. If the radar is directed toward the $\pm x$ -axis, a blocking of communication signals between the ground station and the station and/or VV may occur, as shown in the diagram on the left in Figure 2. Therefore, in this study, we assumed that the station operates with its radar directing toward the $\pm y$ direction, as seen in the diagram on the right.

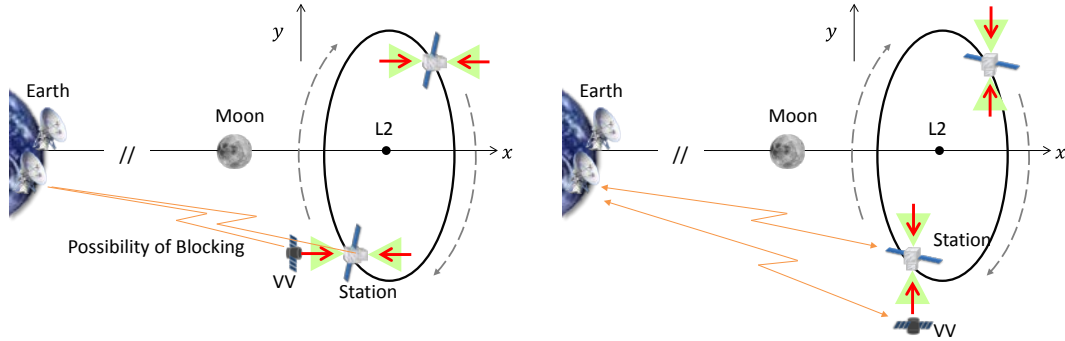


Figure 2. Station attitude with FOV of the onboard radar directing toward $\pm x$ (left) and $\pm y$ (right) directions

4. Navigation Method for EML2 Halo Rendezvous

4.1. Absolute Navigation based on Ground Tracking

Because GPS navigation is for the most part invalid in cis-lunar space, the absolute navigation states of the station and VVs are obtained through ground-based orbit determination. Estimation of the relative state between the station and VV also utilizes these absolute navigation data until the onboard relative navigation sensors begin operation.

In this study, we assumed the use of 2-way Doppler, 3-way Doppler, and data ranging from the Usuda and Uchinoura stations in Japan and NASA's DSN. In order to clarify the forecast precisions of position and velocity in the halo orbit, we conducted orbit determination simulations; the results are shown in Table 1. In the worst case, which corresponds to a 1-day arc length and minimum lunar declination, the precision is 1.05 km (1σ) with respect to position and 1.28 cm/s (1σ) for velocity. We confirmed that these precision values do not change drastically for various locations in the halo orbit. For simplicity, we have adopted the precision of 5 km (3σ) for position and 5 cm/s (3σ) for velocity for the simulation analysis described in later sections.

Table 1. Absolute navigation precision in EML2 halo orbit

Data arc length [day]	1		6	
	Max	Min	Max	Min
Lunar declination				
Position error (1σ) [km]	0.529	1.05	0.806	1.07
Velocity error (1σ) [cm/s]	1.15	1.28	0.397	0.602

4.2. Relative navigation using LOS angle and ranging data

For relative navigation within the range of several hundreds of kilometers from the station, the following two types of data can be utilized: 1. line-of-sight (LOS) angle data measured by the onboard visible cameras and 2. ranging data obtained via the ranging function of the proximity communication equipment onboard both the station and VV (hereafter, PROX ranging).

From the H-II Transfer Vehicle (HTV) experience, it is expected that the proximity communication link will be established within a 200-km distance. Therefore, we assumed that PROX ranging data can also be obtained from 200 km. In order to examine the valid range of a visible camera, we conducted visibility analysis based on the modeling method proposed by Yamamoto et al. [9]. By assuming commonly used camera specifications and the optical properties of spacecrafts, we confirmed that visible cameras can be utilized at distances greater than 200 km in the halo orbit. In this study, for simplicity, we assumed that both the PROX ranging and visible cameras begin their measurements from a relative distance of 200 km.

4.3. Relative Navigation using Lidar

We expect that the station will be equipped with laser reflectors around the docking mechanism for cooperative rendezvous. Therefore, as a relative navigation sensor within a range of several hundreds of meters from the station, we can utilize a Lidar which is equivalent to the rendezvous sensor (RVS) that is used on HTV [10], which measures the LOS angle and range with respect to the laser reflectors. The valid range is assumed to be approximately 600 m.

5. Trajectory Safety

Current ISS trajectory safety policies would also be adopted for cis-lunar rendezvous, after appropriate modifications and/or expansion. The ISS trajectory safety is ensured by the concepts of the Approach Ellipsoid (AE) and the Keep Out Sphere (KOS). AE is an ellipsoid with dimensions of $4 \text{ km} \times 4 \text{ km} \times 2 \text{ km}$ and KOS is a 200-m radius sphere, both centered at the ISS center of mass. Visiting vehicles must not enter AE prior to the approach initiation (AI) maneuver, and all burns performed by VVs must provide coast trajectories that remain outside AE, including its three-sigma dispersion area, for at least 24 h. After the AI maneuver, all burns must be targeted to result in an at least a 4-orbit safe coast trajectory without entering KOS. These requirements can be interpreted so that passive aborts should be safe. In addition, KOS may be entered only in the predefined corridor specified for the particular VV.

In a cis-lunar rendezvous operation, it would be preferable that ground operators perceive few differences from the current ISS-rendezvous operations. Just as ISS has strictly defined rules regarding trajectory safety, the cis-lunar station would impose similar constraints on VVs. In this study, we applied the same ISS rules for cis-lunar rendezvous. However, AE is

not necessarily ellipsoid because the relative motion in cis-lunar space is almost rectilinear and does not form a 2:1 ellipse as in LEOs. Thus, we adopted the Approach Sphere (AS) with a radius of 2 km to replace AE. The design of approach corridor should consider VV's GN&C performance. However, in this study, we defined a cone-shaped region with a cone angle of $\pm 5^\circ$, which corresponds to the size of the nominal corridor of HTV [10].

Because the station performs active navigation with its onboard radar, this corridor should be included within the radar FOV. Thus, we assumed that the corridor extends in the same direction as the station-based radar, that is, in the $+y$ or $-y$ direction.

6. Design and Analysis of the Rendezvous Trajectory

6.1. Trajectory Design

In this study, we designed a VV approach trajectory from an LEO departure to its arrival at a point 30 m from the station.

The trajectory was designed in consideration of the following four guidelines:

1. Passive abort should be safe, that is, the 24-h drift trajectory after a cancelation of any planned maneuver should not enter into the safety regions, and the final approach trajectory should be within the predefined corridor.
2. The VV should approach the station within FOV of the station-based radar.
3. Fuel consumption and the total flight time should be reasonable.
4. Timings of operational events, such as maneuvers and the evaluation of navigation data, should be practical from the perspective of real flight operation.

Regarding maneuvers that are planned on the basis of absolute navigation, in view of previous mission analyses, we assumed that 24 h would be needed for orbit determination and maneuver planning. As for maneuvers that do not require ground operations, we adopted a minimum 6000-s interval.

6.2. Overview of the Rendezvous Scenario

In this section, we briefly introduce the overall rendezvous operation scenario. Details regarding the design and analysis are provided in the following sections.

The scenario is divided into four phases: 1. transfer phase, 2. far-approach phase, 3. rendezvous phase, and 4. proximity phase. Figure 3 shows an overview of the rendezvous operation scenario.

First, in the transfer phase, VV departs from LEO, swings by the Moon, and is inserted into the halo orbit at a certain distance from the station. Three major maneuvers are conducted

to achieve this transfer: an LEO departure, a lunar swing-by, and a halo orbit insertion. In this study, the insertion point is set at the point furthest from the Earth, where both the flight time and ΔV cost are reasonably low. In this phase, the navigation state is determined by a ground-based tracking system and the maneuver planning is conducted by ground operators.

Second, in the far-approach phase, VV first corrects for orbit insertion error and then approaches the point at a relative distance of approximately 200 km, at which the proximity communication between the station and VV is established and both the onboard visible camera and PROX ranging begin measurement. At the same time, the station-based radar also initiates operation. While evaluating the relative navigation data, VV slowly moves to the 100-km point.

Third, in the rendezvous phase, evaluation of the relative navigation data has been completed and the navigation method switches from ground-based absolute navigation to onboard relative navigation. The control maneuvers in this phase are planned onboard the spacecraft. In this phase, VV passes through several intermediate points and arrives at a point 500 m away from the station. On the way to the 500-m point, the onboard Lidar is initiated and data evaluation is completed by the time of the 500-m arrival.

Finally, in the proximity phase, the relative navigation method switches from PROX ranging and LOS angle measurement to Lidar. VV nears the 30-m distance from the station, where the docking operation starts. Closed-loop trajectory control is applied in this phase.

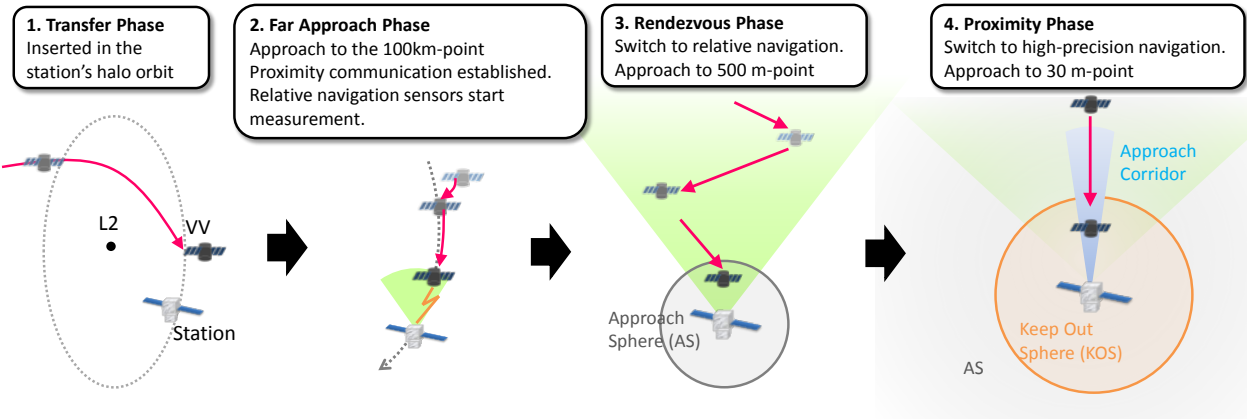


Figure 3. Overview of the rendezvous operation

The details of each phase are described in the following sections.

6.3. Transfer Phase

6.3.1. Trajectory Design for Transfer Phase

In the transfer phase, the visiting vehicle departs LEO and enters into the station's orbit at a certain distance from the station. Since the station is so far from VV, guidance can be conducted without considering the station's real-time state. VV is simply guided so that it travels along the predefined trajectory.

For the transfer, we selected the three-impulse transfer method using a lunar gravity assist, for which ΔV costs are reasonably low and flight time is short, as proposed by Mingtao and Jianhua [11]. Using this method, maneuvers are conducted upon departing LEO, when flying by the Moon, and when being inserted into the destination orbit. In this study, the insertion point is fixed at the point furthest from the Earth, where both the flight time and ΔV cost are reasonable.

First, we computed the ideal trajectory of VV using the optimization method known as Sequential Quadratic Programming (SQP). Here we assumed the LEO parking orbit to have an altitude of 250 km and an inclination of 30.16° . The lunar flyby maneuver is conducted 100 km above the lunar surface. Figure 4 illustrates the designed trajectory with the maneuver points denoted by open circles. TLI, PLSB, and HOI are abbreviations for trans-lunar injection, powered-lunar swing-by, and halo orbit insertion, respectively. The first two trajectory correction maneuvers (TCMs), TCM1 and TCM2, are performed 24 h after TLI and 24 h before PLSB, respectively, both attempting to arrive at the preplanned position of PLSB. We conducted TCM3 24 h after PLSB, aiming to arrive at the preplanned position of HOI.

The flight time from TLI to PLSB is 4.77 days and that from PLSB to HOI is 2.96 days. The flight time in the transfer phase totals 7.73 days.

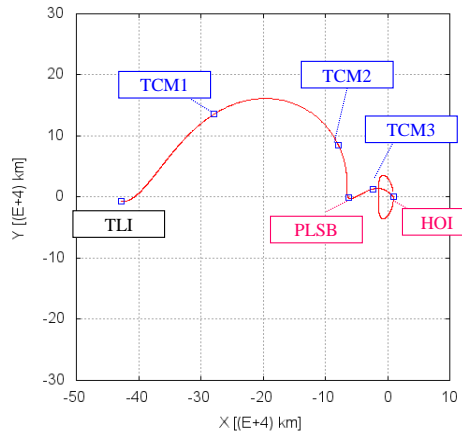


Figure 4. Transfer trajectory as viewed in the Earth–Moon rotating frame

6.3.2. Simulation for Transfer Phase

We ran a Monte Carlo simulation 100 times to examine the GN&C performance. These simulation model results are summarized in Table 2 and Table 3. The initial state error at TLI was estimated on the basis of the rocket insertion error. The navigation errors at each maneuver point were obtained from the software simulation results using the same tracking stations described in section 4.1. Maneuver execution errors of 1.0% (3σ) magnitude and 1° (3σ) pointing direction were considered.

Table 2. Simulation model summary for the transfer phase

Orbit propagation	Full ephemeris (DE405) Sun, Earth, Moon , point mass
Initial state error at TLI	$\sigma_a = 5.576e + 2$ km, $\sigma_e = 2.397e-4$, $\sigma_i = 5.391e-3^\circ$, $\sigma_\Omega = 1.114e-1^\circ$, $\sigma_\omega = 9.849e-2^\circ$, $\sigma_M = 3.569e-3^\circ$
Navigation	Ground-based absolute navigation Accuracy: see Table X
Guidance	Implicit fixed time arrival guidance
Maneuver	Impulsive maneuver Execution error: 1.0% (3σ) in magnitude, 1° (3σ) in pointing

Table 3. Absolute navigation error in transfer phase

Navigation error (1σ)	TCM1	TCM2	PLSB	TCM3	HOI
Position [km]	0.820	4.532	0.817	0.548	1.474
Velocity [cm/s]	0.787	4.213	51.022	0.688	1.595
Data arc length [h]	19	62.5	20	20	43

Table 4 summarizes the simulation. The mean total ΔV cost is 346.85 m/s. The position and velocity errors with respect to the pre-planned HOI point are around 27 km (3σ) and 5 m/s (3σ) for the worst axis, respectively.

Table 4. Simulation results of the transfer phase

	ΔV [m/s]		Time from TLI [day]
	mean (μ)	3σ	
TCM1	8.343	10.527	1
TCM2	0.218	0.501	3.77
PLSB	189.771	4.491	4.77
TCM3	9.353	20.4	5.77
HOI	139.161	4.782	7.73
Total ΔV [m/s]	mean:346.85, 3σ : 40.70		
Total flight time [day]	7.73		

Perilune altitude [km]	109.265($\mu-3\sigma$)
Position error at HOI [km]	dx = 17.07, dy = 23.13, dz = 26.37 (3σ)
Velocity error at HOI [m/s]	dvx = 4.17, dvy = 5.07, dvz = 1.11 (3σ)

6.4. Far-Approach Phase

6.4.1. Trajectory Design for Far-Approach Phase

The far-approach phase begins after the HOI maneuver, and its destination is a location point 100 km away from the station.

When considering the distance from the station at which VV should be inserted, we must take into account the 24-h trajectory safety. Given that the next maneuver would be performed 24 h after the HOI maneuver, the HOI point should be designed such that the total 48-h free-drift trajectory will never enter the Approach Sphere (AS) of the station. To meet this requirement, we designed the HOI point to be located 1,000 km away from the station. In this study, we set the HOI point to be “behind” the station when viewed in the Earth–Moon rotating frame, which results in the VV approaching the station from the +y direction.

The VV first corrects the HOI insertion error and then begins its approach. On the way to the 100-km destination, VV travels around an intermediate point located 200 km away from the station, where both the station-based and the VV-based relative navigation sensors start their measurements. By evaluating the PROX-ranging and LOS-angle measurement data, VV gradually approaches the destination. In this study, we designed the 100-km and 200-km points to be located (80.0, 173.0, 0.0) km and (20.0, 70.0, 0.0) km, respectively. These points are designed so that the 24-h free-drift trajectories would never enter AS.

Figure 5 illustrates the relative trajectories of VV with respect to the station, as viewed from the station-centered Earth–Moon rotating frame. The blue line, starting from the blue asterisk, shows the ideal 3-day drift trajectory, which VV would follow if it were inserted exactly 1,000 km behind the station. The pink line is an example of a simulated VV trajectory. The yellow, green, and purple dots, labeled HOI, TCM4, and V0, indicate the insertion point, correction maneuver point, and approach starting point, respectively. As described in this figure, VV shifts toward the ideal trajectory after TCM4 and then approaches the station. The blue and orange dots labeled V1 and V2 indicate the 200-km intermediate point and 100-km destination point, respectively.

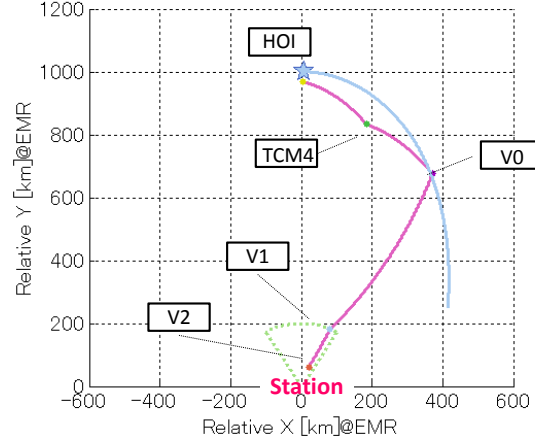


Figure 5. Relative trajectory in the far-approach phase

As mentioned above, we assumed that the orbit determination and maneuver planning will require 24 h for each ground-based maneuver. Thus, the time interval between each maneuver corresponds to 24 h. As for the time duration between the 100-km point (V1) and the 200-km point (V2), we assigned 5 h, which seems sufficient for completing the evaluation of the obtained relative sensor data.

6.4.2. Guidance in Far-Approach Phase

Targeting of the V1 and V2 maneuvers is conducted on the basis of the relative dynamics model described in section 2. Provided that the relative position and velocity of the VV at time t_0 is $[\delta \mathbf{r}_{t_0}, \delta \mathbf{v}_{t_0}]^T$ and the maneuver velocity $\Delta \mathbf{V}_{t_0}$ changes the relative state into $[\delta \mathbf{r}_{t_1}, \delta \mathbf{v}_{t_1}]^T$ at time $t_1 = t_0 + \Delta t$, the solution can be expressed as follows:

$$\begin{bmatrix} \delta \mathbf{r}_{t_1} \\ \delta \mathbf{v}_{t_1} \end{bmatrix} = \Phi(t_1, t_0) \begin{bmatrix} \delta \mathbf{r}_{t_0} \\ \delta \mathbf{v}_{t_0} + \Delta \mathbf{V}_{t_0} \end{bmatrix}$$

Thus, the maneuver velocity required to achieve the desired relative state after Δt is computed as follows:

$$\Delta \mathbf{V}_{t_0} = \Phi_{12}^{-1} (\delta \mathbf{r}_{t_1} - \Phi_{11} \delta \mathbf{r}_{t_0}) - \delta \mathbf{v}_{t_0}$$

where

$$\Phi = \begin{bmatrix} \Phi_{11} & \Phi_{12} \\ \Phi_{21} & \Phi_{22} \end{bmatrix}$$

To minimize linearization error, STM was computed by integrating the differential equations in Eqs. (1) and (3).

6.4.3. Simulation for the Far-Approach Phase

We ran 300 Monte Carlo simulations to evaluate VV performance. A summary of the simulation model results is shown in Table 5. The simulation was performed on the basis of the CRTBP model. We set the initial state errors with respect to the planned position and velocity after HOI of 27 km and 5 m/s (3σ) for each axis, respectively. The navigation errors considered for both the station and VV are 5 km (3σ) for position and 5 cm/s (3σ) for velocity, with reference to the simulation results described in section 4.1.

Table 5. Simulation model summary for the far-approach phase

Orbit propagation	Circular restricted three-body problem
Initial state error at HOI	Position: 27 km (3σ), velocity 5m/s (3σ) for each axis
Navigation	Ground-based absolute navigation for both the station and VV Accuracy: position 5 km (3σ), velocity 5 cm/s (3σ) for each axis
Guidance	Fixed-time arrival guidance STM computed by integration
Maneuver	Impulsive maneuver Execution error: 1.0% (3σ) in magnitude, 1° (3σ) in pointing

Figure 6 shows the computed trajectories as viewed within the station-centered Earth–Moon rotating frame. Table 6 is a summary of the ΔV cost and flight times. The total flight time in this phase is 3.21 days, and the mean total ΔV cost is 9.23 m/s.

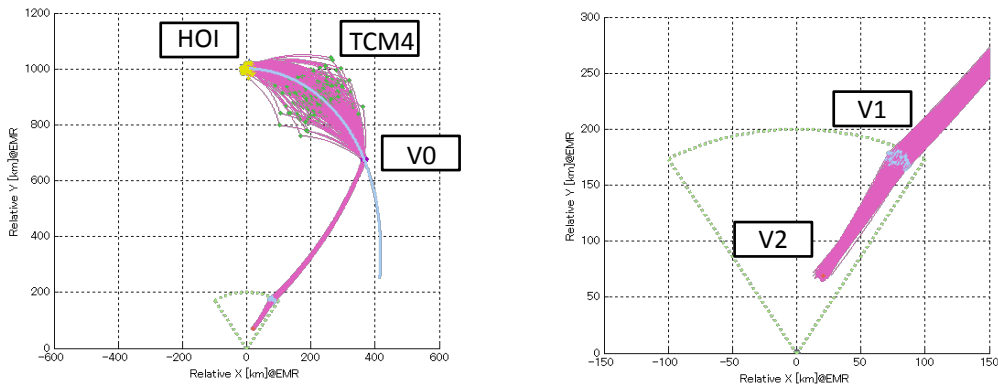


Figure 6. Monte Carlo simulation results (far-approach phase)

Table 6. Simulation results of the far-approach phase

	Relative position [km]	ΔV [m/s]		Time from HOI[day]
		mean (μ)	3σ	
TCM4	-	1.62	2.56	1
V0	-	5.08	1.64	2
V1	(80, 173, 0)	2.53	0.79	3
V2	(20, 70, 0)	-	-	3 + 5 h
Total ΔV [m/s]	mean: 9.23, 3σ : 4.99			
Total flight time [day]	3.21 (3 day + 5 h)			
Position error at V1 [km] (μ + 3σ)	dx = 4.39, dy = 10.73, dz = 11.61			
Position error at V2 [km] (μ + 3σ)	dx = 8.75, dy = 5.13, dz = 8.44			

As shown in Figure 6, the trajectory is almost rectilinear but has a slight clock-wise motion due to the weak Coriolis force. It would be safer to design the trajectory so that VV passes the station on the left.

To confirm trajectory safety, we checked the 24-h free-drift trajectories when the planned maneuver could not be performed due to various anomalies. As Figure 7 shows, the 24-h free-drift trajectories never entered AS of the station.

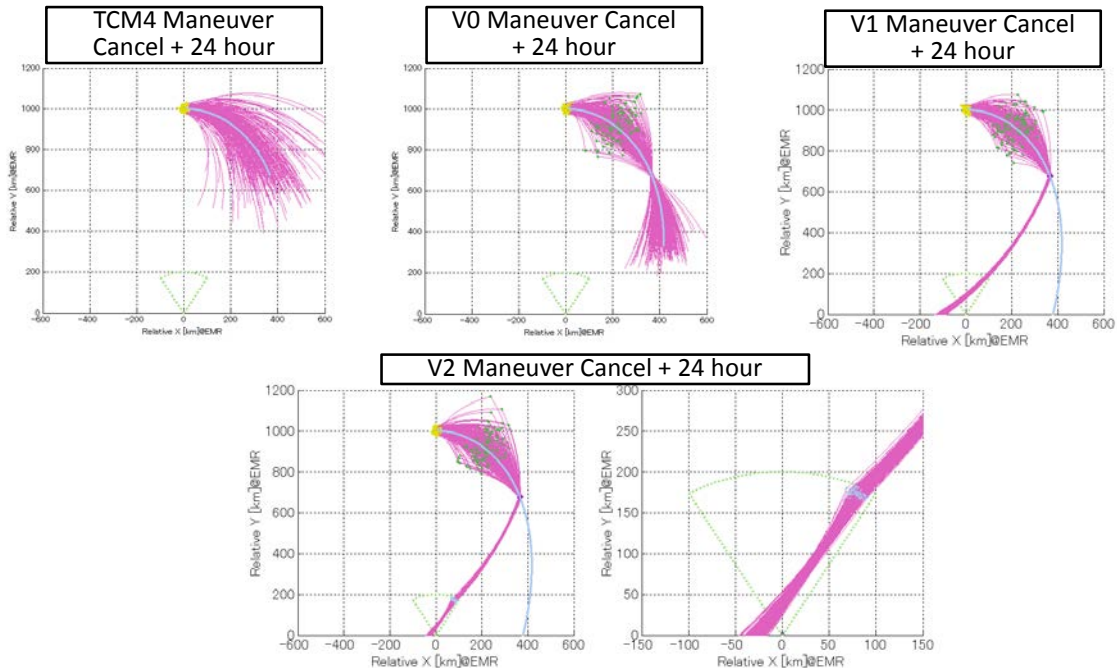


Figure 7. Confirmation of the 24-h free-drift trajectory (far-approach phase)

However, as you can suggest from the top-left plot, the free-drift trajectory after HOI has a possibility of collision if it drifts for a few more days. Actually, it would be preferable to modify the insertion point so that VV would never collide with the station, which we discuss in another work [12].

6.4.4. Hand-over from Absolute Navigation to Relative Navigation

The navigation hand-over from ground-based absolute navigation to onboard relative navigation is a critical event. In order to initiate relative navigation smoothly, VV has to come within the effective measurement ranges of the camera and PROX ranging as planned. In addition, VV has to point toward the station precisely so that it captures the station in the camera's view.

As shown in Figure 6, VV arrived at the 200-km point within the acceptable error range. Regarding the camera view, given that the absolute position of both the station and VV can be estimated with an accuracy of 5 km (3σ) for each axis, the uncertainty of the pointing angle is expected to be $\arctan\left(\text{RSS}\left(5\sqrt{2}, 5\sqrt{2}\right) \text{ km} / 200 \text{ km}\right) \approx 3^\circ$. Thus, if FOV of the onboard camera is greater than $\pm 3^\circ$, VV can capture the station in its camera view. In our design, the camera FOV is expected to be 10–20°; therefore, the navigation hand-over is achievable.

6.5. Rendezvous phase

6.5.1. Trajectory Design for the Rendezvous Phase

In the rendezvous phase, VV approaches the destination at a distance 500 km from the station, located on the $+y$ axis, which we call KOS Initiation (KI) point. The KI point is the starting point for entering KOS. As seen in Figure 8, we have defined another four intermediate points on the way to the KI point so that VV moves in a zigzag manner within FOV of the station-based sensor. We named these points V3, AI, V4, and V5. As the name implies, the AI point is the starting point for entering AS. The locations of these points were designed in consideration of 24-h free-drift safety and are listed in Table 7.

As mentioned in section 6.1, we set a time interval of 6000 s between these maneuver points.

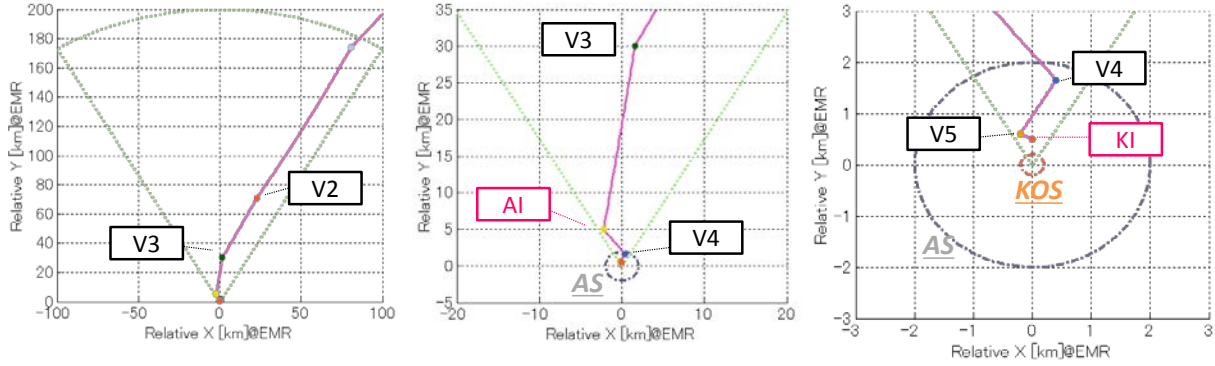


Figure 8. Relative trajectory in the rendezvous phase

Table 7. Maneuver points in the rendezvous phase

Maneuver point	Relative position w.r.t. station [km]
V3	(2, 30, 0)
AI	(-2, 5, 0)
V4	(0.4, 1.5, 0)
V5	(-0.2, 0.6, 0)
KI	(0, 0.5, 0)

6.5.2. Guidance in the Rendezvous Phase

Maneuver targeting is conducted on the basis of the onboard relative navigation data, which utilize PROX ranging and LOS angle measurement data.

The targeting algorithm is almost the same as that in the far-approach phase, which is explained in section 6.4.2. However, in the rendezvous phase, a constant STM is used for fast onboard computation. Because the relative distance is close enough in this phase, STM can be approximated as in Eq. (4). In addition, we simplified STM by applying a constant value to the station position, which we estimated to be the bottom-end point of the halo orbit.

6.5.3. Simulation for the Rendezvous Phase

In total, 300 Monte Carlo simulations were run to evaluate VV's performance. A summary of the simulation model results is shown in Table 8. For the initial state for each run, we used the simulation result of the far-approach phase. The navigation errors at each maneuver point were obtained from the result of the navigation simulation (Table 9).

Table 8. Simulation model summary for the rendezvous phase

Orbit propagation	Circular restricted three-body problem
Initial state at V2	Used the result from the far-approach phase
Navigation	Relative navigation using PROX ranging and LOS angle Accuracy: see Table 9
Guidance	Fixed-time arrival guidance, constant STM
Maneuver	Impulsive maneuver Execution error: 1.0% (3σ) in magnitude, 1° (3σ) in pointing

Table 9. Navigation accuracy of LOS angle- and PROX ranging-based navigation

Relative distance [km]	Position error [m] (3σ)	Velocity error [cm/s] (3σ)
200–100	60.0	5.0
100–50	30.0	3.0
50–10	10.0	1.0
10–1	5.0	0.5
1–0.5	1.5	0.2

Figure 9 and Table 10 show the simulation results. The total flight time in this phase is 0.35 days (8.3 h), and the mean total ΔV cost is 9.81 m/s. The total dispersion at the KI insertion point is about 27 m (3σ), which is within the $\pm 5^\circ$ cone of the approach corridor. As shown in the figure, VV remains within FOV of the station-based radar during this phase.

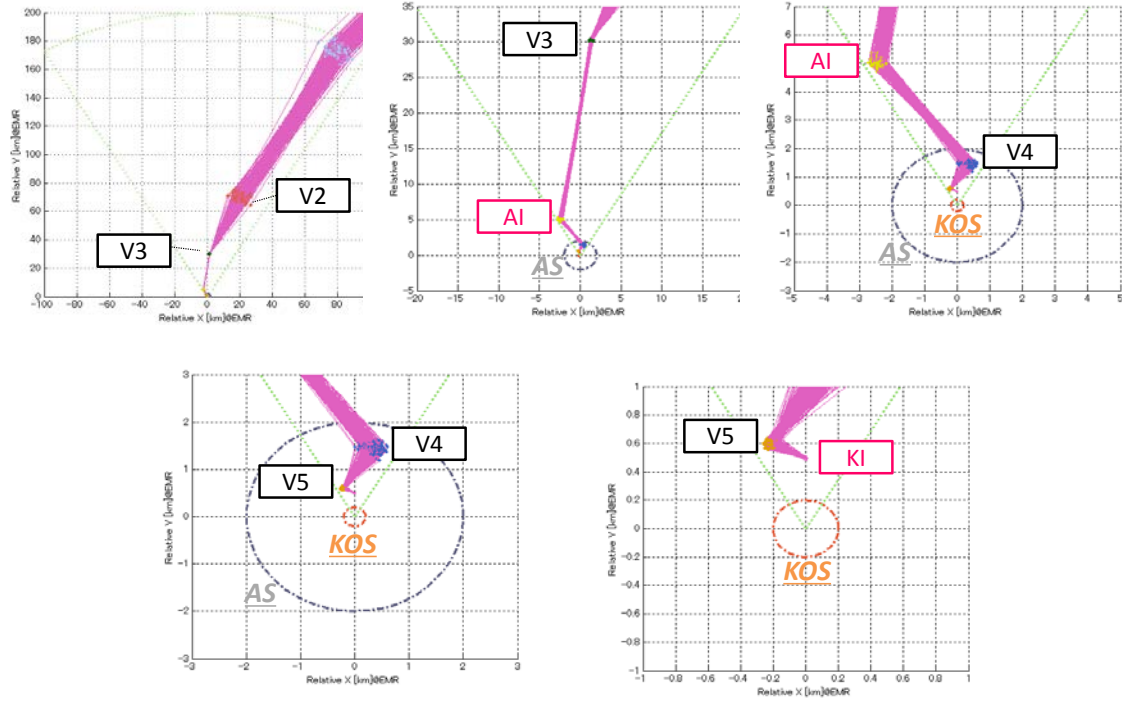


Figure 9. Monte Carlo simulation results (rendezvous phase)

Table 10. Simulation results for the rendezvous phase

	Relative position [km]	ΔV [m/s]		Time interval [min]
		mean (μ)	3σ	
V2	(20, 70, 0)	1.49	1.54	100
V3	(2, 30, 0)	3.64	1.11	
AI	(-2, 5, 0)	3.79	0.11	
V4	(0.4, 1.5, 0)	0.71	0.11	
V5	(-0.2, 0.6, 0)	0.18	0.04	
KI	(0, 0.5, 0)	-	-	
Total ΔV [m/s]	mean: 9.81, 3σ : 2.91			
Total flight time [day]	0.35 (= 8.3 h)			
Position error at KI [m] (μ , 3σ)	dx: $\mu = -2.47$, $3\sigma = 14.53$ dy: $\mu = -3.20$, $3\sigma = 15.58$ dz: $\mu = -0.05$, $3\sigma = 16.76$			

In order to check the trajectory safety, we confirmed the 24-h free-drift trajectories. As shown in Figure 10, the free-drift trajectories up until the AI maneuver never enter AS and those after the AI maneuver do not penetrate KOS.

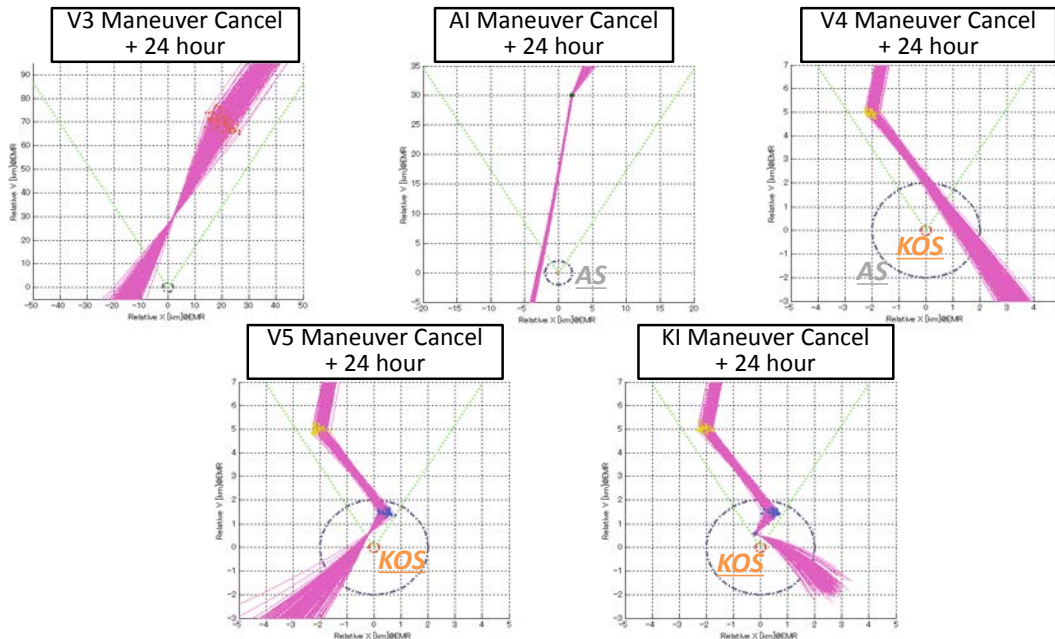


Figure 10. Confirmation of the 24-h free-drift trajectory (rendezvous phase)

6.6. Proximity phase

In the proximity phase, VV approaches the 30-m point along the y -axis via the approach corridor. This approach is similar to the R-bar approach of HTV [10]. Continuous closed-loop control is performed by Lidar relative navigation. The position and velocity is controlled such that VV aligns with the predefined approach profile. The PD controller generates thruster firing commands on the basis of the difference between the navigation data and guidance data.

As seen from the previous discussion, the relative dynamics in the EML2 halo orbit are almost rectilinear; therefore, an approach via a predefined corridor is reasonably achievable. However, because the direct approach has a great risk of collision, fault detection, isolation, and recovery (FDIR) and active abort functions should be specially designed for this environments.

Provided that the total operation time is set to 4000 s, the total ΔV cost is estimated to be about 2.3 m/s [13].

6.7. Summary of the Rendezvous Trajectory Design

Table 11 summarizes the total mean ΔV and flight times for all phases. The total ΔV cost and flight time are 368.2 m/s and 11.33 days, respectively, which would be acceptable for the expected logistics mission system. Given that the operation duration after halo orbit insertion is 3.60 days and the insertion point is located at the point furthest from the Earth, we can see that the rendezvous point is located around the bottom end of the halo orbit.

Table 11. Summary of the ΔV and flight time

Phase	Relative range [km]	ΔV (mean) [m/s]	Flight time
Transfer	-1,000	346.85	7.73 day
Far-approach	1,000-100	9.23	3.21 day
Rendezvous	100-0.5	9.81	8.3 h
Proximity	0.5-0.01	2.3	4000 sec
Total		368.2 (22.0 in EML2 halo)	11.33 day (3.60 day in EML2 halo)

The 24-h free-drift safety was confirmed in both the far-approach and rendezvous phases, and the hand-over from ground-based absolute navigation to onboard relative navigation was confirmed to be achievable. As we mentioned in section 3.3, the station-keeping maneuver would be performed when the station crosses the x-z plane; thus, the station would not perform any station-keeping operation such as attitude changes and translational controls during VV's rendezvous operation.

7. Issues to Consider regarding the EML2 Halo Orbit Rendezvous

In this study, we developed a feasible rendezvous scenario. However, there are a number of unfixed assumptions to be examined in future research.

First is the configuration and operational scenario of the station. We assumed that the station is to be operated at a fixed attitude in the Earth-Moon rotating frame and the approach corridor is directed toward the +y or -y axis in view of the availability of ground communication. However, the station attitude should be defined with consideration of not only ground communication but also power generation, regular and irregular operations such as station-keeping maneuvers, and scientific observations, among others. If the station attitude changes, the approach trajectory must also change.

Second is the station-based navigation sensor assumption. Since we assumed that the station conducts relative navigation with its onboard radar, the trajectory was designed so that VV flies within the $\pm 30^\circ$ FOV of the station-based radar. However, the requirement

from the station-based sensor is not clarified yet and it is not certain whether the station would install such an active navigation sensor.

Third is the insertion point assumption. In this study, the insertion point was assumed to be the point furthest from the Earth, in view of striking a balance between the ΔV cost and flight time. However, this is not the only point where VV can arrive at a reasonable ΔV cost and flight time. There are other possible locations where VV could be inserted in the halo orbit. If the insertion point changes, the approach direction would also change. In addition, whether VV is inserted in front of or behind the station would also affect the approach direction.

Fourth is the definition of the safety region. We sized AS and KOS with reference to AE and KOS of ISS. However, an appropriate safety region should be designed considering the actual approach trajectory. In addition, the safety requirement, such as 24-h drift trajectory safety, may also require modification for cis-lunar rendezvous.

Time limitations should also be considered in detail. For unmanned missions, a total operation time of 11.33 days would be acceptable. However, for manned missions, time limitation is a critical issue whereby shorter rendezvous durations would be preferable. Regarding this point, we consider that there is much room for improvement in the total operation time after halo-orbit insertion. As seen from the previous discussion, the key operation that takes the most time is the ground-based absolute orbit determination, which we assumed to be 24 h in this study. In fact, we suppose that this period could be shortened to half a day or so, with only an insignificant decrease in the precision. Moreover, it may be possible to shorten it drastically if a feasible trajectory could be obtained despite a decrease in the precision. In addition, the HOI point can be shifted much closer to the station with 24-h free-drift safety being ensured, which results in shorter flight time during the far-approach phase.

Sun direction would also affect the trajectory design. We should determine the VV's approach direction so that the direct sunlight would not interfere sensor measurements.

These unfixed matters should be examined in future work. Parametric studies on this rendezvous strategy will help to reveal the operational requirements and to determine details for the configuration and /or operation scenarios of the future cis-lunar station.

8. Conclusions

This work addressed the practical rendezvous scenario design in which an unmanned logistics transfer vehicle rendezvous with a future cis-lunar station in an EML2 halo orbit. Based on several assumptions regarding the operational constraints, configuration, and operational scenario of the station, we confirmed that VV could reach a distance 30 m from

the station with an acceptable ΔV cost and flight time. In addition, we also confirmed that trajectory safety could be maintained during the rendezvous operation. However, regarding the assumptions which were used in this study, there are still many issues to be considered. It is important that other parametric cases be studied and the requirements for the VV and station be developed, which we plan for our future work.

9. Acknowledgments

We would like to express our sincere gratitude to the Fujitsu Japan Ohnishi Team for its well-considered ground-based navigation analysis. We would also like to thank Mitsubishi Electric Corporation and NEC Corporation for supporting the technical aspects of the GN&C design.

10. References

- [1] International Space Exploration Coordination Group, "The Global Exploration Roadmap," August 2013.
- [2] Gates, M., Mazanek, D., Muirhead, B., Stich, S., Naasz, B., Chodas, P., McDonald, D., and Reuter, J., "NASA's Asteroid Redirect Mission Concept Development Summary," IEEE Aerospace Conference, March 2015.
- [3] Gomez, G., Koon, W. S., Lo, M. W., Marsden, J. E., Masdemont, J., and Ross, S. D., "Invariant Manifolds, the Spatial Three-Body Problem and Space Mission Design," AIAA/AAS Astrodynamics Specialist Meeting, Quebec City, Canada, 2001, Paper No. AAS 01-301.
- [4] Lo, M. and Ross, S., "The Lunar L1 Gateway: Portal to the Stars and Beyond," AIAA Space 2001 Conference and Exposition, Albuquerque, New Mexico, 2001.
- [5] Howell, K. C., and Kakoi, M., "Transfers between the Earth-Moon and Sun-Earth systems using manifolds and transit orbits," *Acta Astronautica*, Vol. 59, pp. 367-380, 2006.
- [6] Kakoi, M., Howell, K. C., and Folta, D., "Access to Mars from Earth-Moon Libration Point Orbits: Manifold and Direct Options," Proceedings of the 64th International Astronautical Congress, Beijing, China, 2013, Paper No. Paper IAC-13-C1.7.12.
- [7] Mand, K., Woffinden, D., Spanos, P., and Zanetti, R., "Rendezvous and Proximity Operations at the Earth-Moon L2 Lagrange Point: Navigation Analysis for Preliminary Trajectory Design," AAS 14-376.
- [8] Folta, D.C., Woodard, M., Pavlak, T., Haapala, A., and Howell, K.C. (2012), "Earth-Moon Libration Stationkeeping: Theory, Modeling, and Operations," 1st IAA/AAS

Conference on the Dynamics and Control of Space Systems, Porto, Portugal, March 19-21, 2012.

[9] Yamamoto, T., Murakami, N., Nakajima, Y., and Yamanaka, K., “Navigation and Trajectory Design for Japanese Active Debris Removal Mission,” Proceedings of the 24th International Symposium on Space Flight Dynamics (ISSFD), Laurel, Maryland, 2014.

[10] Ueda, S., Kasai, T., and Uematsu, H., “HTV Rendezvous Technique and GN&C Design Evaluation Based on 1st Flight On-orbit Operation Result,” Proceedings of the AIAA/AAS Aerodynamics Specialist Conference, Toronto, Ontario, Canada, August, 2010.

[11] Mingtao, L., Jianhua, Z., “Impulsive lunar Halo transfers using the stable manifolds and lunar flybys,” Acta Astronautica, Volume 66, Issues 9–10, 2010, pp. 1481–1492.

[12] Ueda, S. and Murakami, N., “Optimum Guidance Strategy for Rendezvous Mission in Earth-Moon L2 Halo Orbit,” Proceedings of the 25th International Symposium on Space Flight Dynamics (ISSFD), Munich, Germany, 2015.

[13] Kitamura, K., Sato, Y., Hotta, S., Murakami, N., Ueda, S., and Yamamoto, T., “Rendezvous trajectory in the vicinity of the Space Station on EML2,” Proceedings of the 24th Workshop on Astrodynamics and Flight Mechanics, Sagamihara, Kanagawa, Japan, July, 2015.